Near-surface imaging in frozen environments using GPR

Monica Moldoveanu-Constantinescu and Robert R. Stewart

ABSTRACT

This paper describes ground-penetrating radar (GPR) surveys that were conducted to characterize the ice and shallow subsurface of a frozen lagoon at Bowness Park, Calgary. We used Sensors and Software Inc.'s 250 MHz NOGGIN® and SmartCart® system as well as a Pulse EKKO 4 system with a 100 MHz antenna to acquire GPR surveys over the frozen lagoon in two consecutive years (2003 and 2004). Hyperbolic velocity analysis gave ice velocities of about 0.15 m/ns with velocities decreasing in the sediments to about 0.11 m/ns. We interpret the ice thickness to be about 0.4 meters from the GPR profiles, which is consistent with augur holes drilled through the ice. Channel sediments and stratigraphy beneath the ice are interpretable from the 3D radar reflectivity. We located and mapped a paleochannel with a NW-SE orientation and a thickness of about 0.5 meters. Penetration of the 250 MHz data reached about 2 meters at several locations in the area.

INTRODUCTION

Ground penetrating radar (GPR) uses electromagnetic wave propagation and scattering to image, locate and identify changes in electrical and magnetic properties in the ground (Olhoeft, 2000). It can have very high resolution, approaching centimeters under the right conditions. The most commonly used type of GPR survey is common-offset, single-fold reflection profiling. In reflection mode, a GPR instrument is moved along a survey line acquiring responses at regular intervals (Figure 1). These are used to create a cross sectional image of the ground. The procedure involves repetitive moves of both transmitter and receiver at a constant antennae spacing. Processing and plotting of GPR data provides a profile of the horizontally surveyed distance, generally in meters, versus vertical two-way travel time, usually in nanoseconds. The depth of the reflections can be estimated by measuring the electromagnetic wave's propagation velocity in the material under consideration.
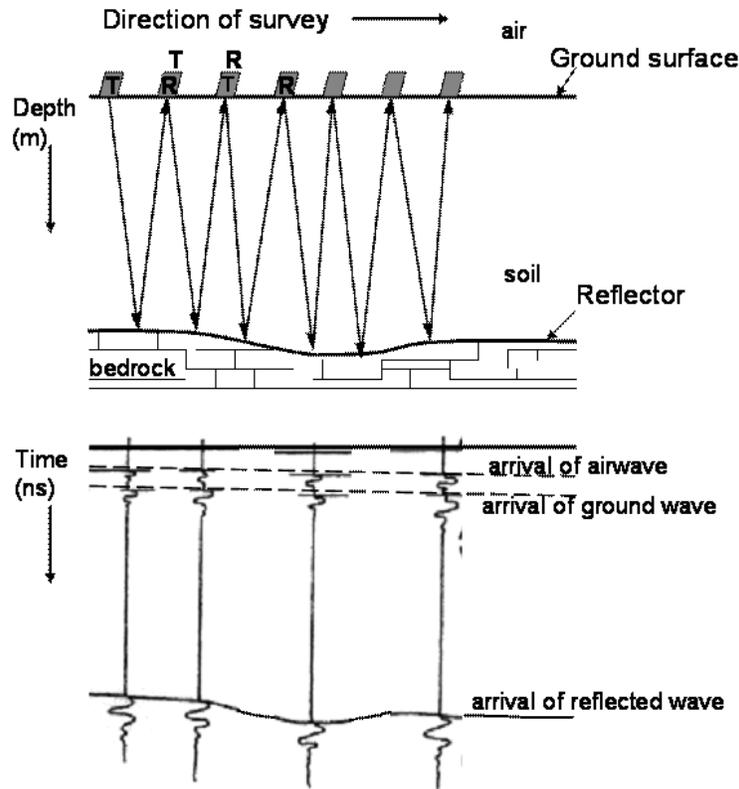
FIG. 1. Schematic illustration of common-offset single-fold profiling, with four schematic GPR traces, showing the arrival of air and ground waves, and a reflected wave from a subsurface reflector.

Ground penetrating radar provides a powerful tool for mapping the thickness of ice - as ice is largely transparent to radio-wave signals and the underlying ice-sediment or ice-water interfaces can be quite reflective. To investigate ice thickness and its underlying sediments, we acquired two quasi-3D GPR surveys on a frozen lagoon at Bowness Park in Calgary (Figure 2). We were interested in determining the ice thickness over the lagoon as well as imaging the fluvial sediment environment beneath the ice. We also acquired several lines over the frozen land north of the lagoon and a common midpoint (CMP) gather with the purpose of performing velocity analysis.

250 MHz NOGGIN and Smart Cart system

FIG. 2. Dr. Larry Bentley and Ms. Julie Aitken of the University of Calgary and Mr. Greg Johnston of Sensors and Software Ltd. conduct a GPR survey, with the Noggin® 250 MHz SmartCart®, over the frozen lagoon at Bowness Park, Calgary**.**

Bowness Park is situated in northwest Calgary, on the south side of the Bow River and covers about 30 hectares of land. Much of the topographic relief in the City of Calgary is a result of Quaternary rivers downcutting through the near-surface Paleocene units. Lithologically and stratigraphically, the area is composed of unconsolidated sediment, mostly tills, glaciolacustrine deposits and alluvium, overlying sandstone and shale (Osborn and Rajewicz, 1998) as it can be seen on the surficial geology map of Calgary (Figure 3).
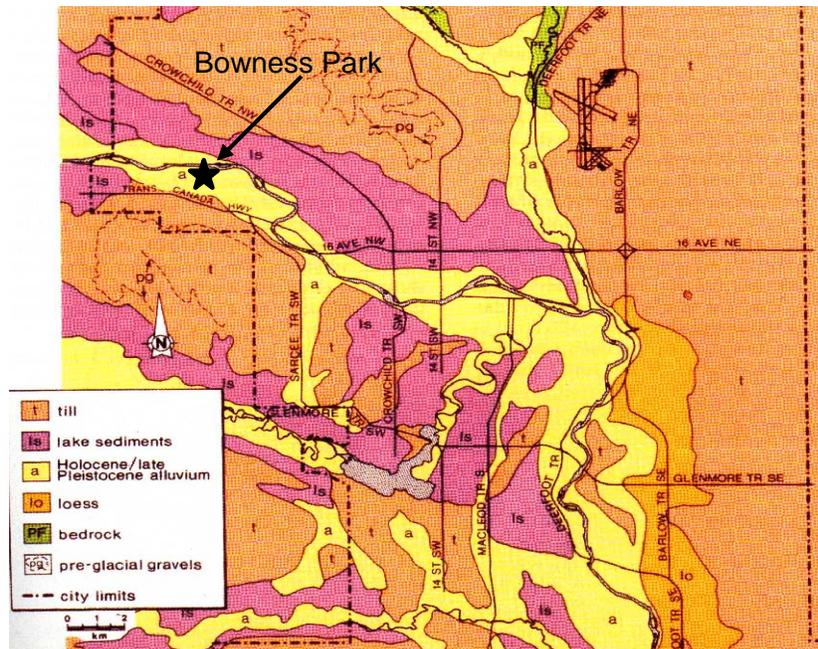
FIG. 3. Surficial geology map of Calgary with the location of the study area (modified after Moran, 1986).

The ice on the lagoon (a popular skating area) is created by first draining the lagoon and then slowly filling it with water that freezes. The GPR surveys were located on the southeast side of the lagoon as illustrated in Figure 4.
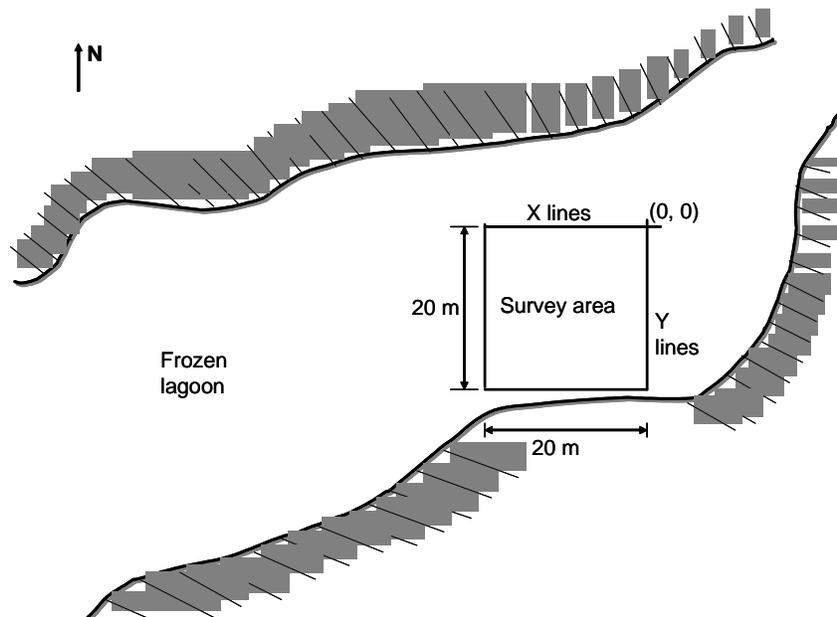
FIG. 4. The location of the GPR surveys on the lagoon at Bowness Park, Calgary.

We acquired a 25 m by 45 m survey in 2003 and a 20 m by 20 m survey in 2004. These surveys consisted of 26 and 42 lines respectively.

To process the data, we used Win EKKO and EKKO Mapper software from Sensors & Software Inc. Plan-view maps of the near-surface structure at different times and depths were computed to analyze the horizontal distribution of the subsurface features. A single line, from the 2003 survey, is shown in Figure 5. We have interpreted the bottom of the ice on this section.
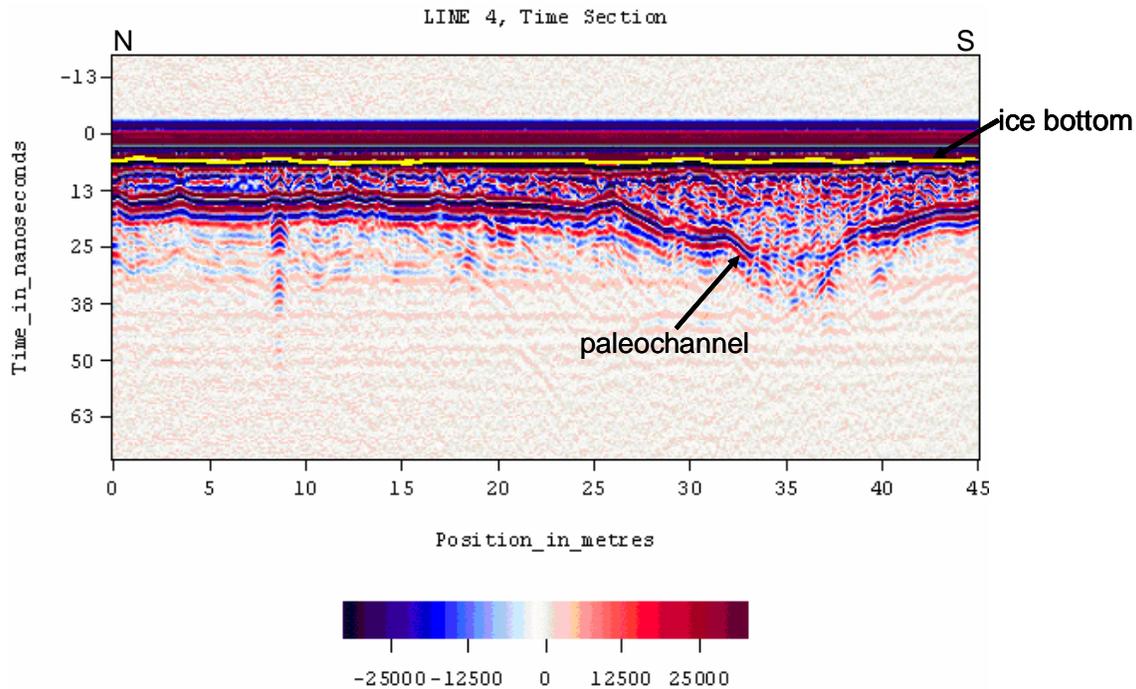
FIG. 5. A 2D line from the survey acquired over the frozen lagoon at Bowness Park. The interpreted ice bottom is indicated in yellow.

SURVEY DESIGN

The purpose of the survey was to structurally image the area, determine the ice thickness, and establish the depth to the bedrock. The type of survey was common-offset, single-fold reflection profiling, with several velocity (CMP) profiles. The surface of the 2003 survey was designed to be 25 m by 45 m. The analysis of the data acquired during the 2003 survey provided information about the location of the paleochannel and determined the design of the 2004 survey. The 2004 survey was more detailed, focused on the area where the paleochannel was located. This survey was designed as a 20 by 20 m grid. A 2D line from this survey is shown in Figure 6.
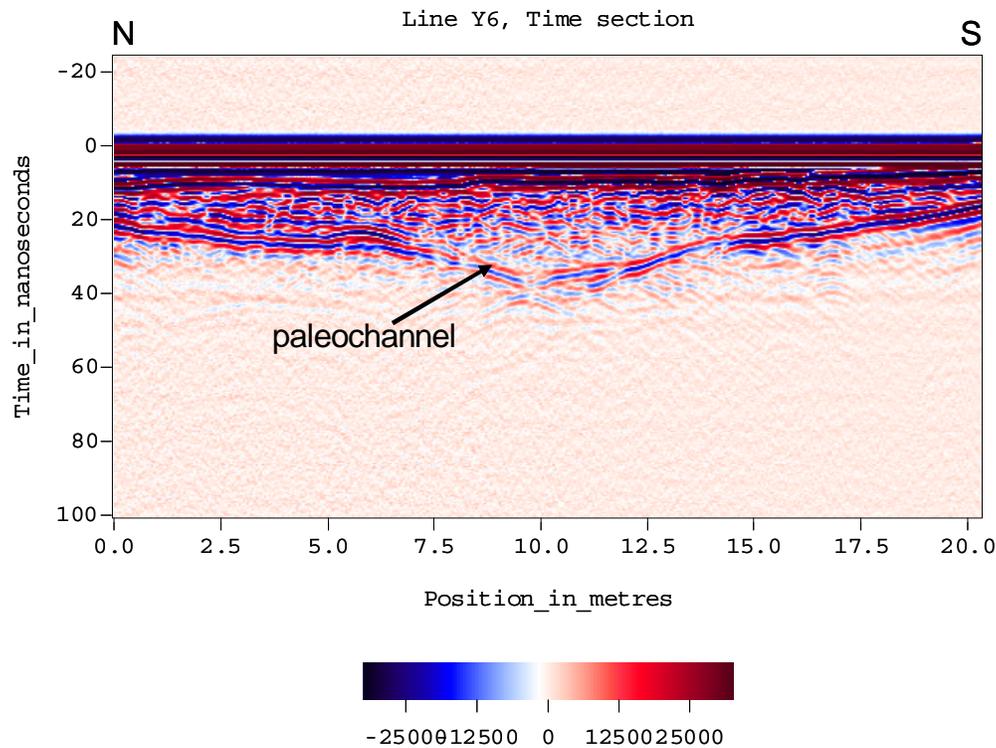
FIG. 6. A 2D line from the more detailed 2004 survey of the channel area.

There are seven parameters to define for the type of survey mentioned above. In order as presented below these parameters are: operating frequency, length of recording time, time sampling interval, station spacing, antennae separation, line location and spacing, and antenna orientation. In this section we will review each of them separately.

1.) In every GPR survey design, there are trade-offs between spatial resolution, depth of penetration and system portability when selecting an operating frequency and station spacing. The centre frequency is selected to be between the value of the frequency for the spatial resolution desired and the value of the exploration depth frequency. In other words, spatial resolution places a lower bound and depth of investigation places an upper bound on the centre frequency. The constraint on the centre frequency takes the form

$$f_c^R > \frac{75}{\Delta Z \sqrt{K}} MHz$$,

(Annan, 2003), where ΔZ is the spatial separation to be resolved in meters and K is the dielectric constant. For a spatial separation of 0.15 m and a dielectric constant of 4 (the dielectric constant of ice has values between 3 and 4) we find that the centre frequency should be at least 250 MHz.

For the exploration depth frequency, the constraint takes the form

$$f_c^D < \frac{1200\sqrt{K-1}}{D} MHz .$$

With a dielectric constant of 4 and an assumed maximum depth of 3 m we see that the centre frequency should be less than 680 MHz.

2.) The expression used to estimate the time length of the record was

$$W = 1.3 \frac{2 \times depth}{velocity} ,$$

where the maximum depth and minimum velocity likely to be encountered in the survey area are used. For an estimated depth of ~3 m, and a velocity of 0.08 m/ns (as determined from the CMP analysis), the recording time window will be 97.5 ns. Therefore, the use of a 100 ns time window should provide enough information for characterizing the subsurface.

3.) The temporal sampling interval represents the time interval between points on a recorded waveform. The sampling interval is controlled by the Nyquist sampling concept and should be at most half the period of the highest frequency signal in the record. The function relationship is

$$t = \frac{1000}{6 f_c} ,$$

where f_c is the centre frequency in MHz and t is the time in nanoseconds. For a frequency of 250 MHz, the temporal sampling interval is 0.66 ns. However, this is the maximum sampling interval. We decided to choose a smaller interval, 0.4 ns.

4.) Station spacing or sampling interval is extremely important and should be considered into the survey design process. In order to assure that the ground response is not spatially aliased, the Nyquist sampling intervals should not be exceeded (Keary and Brooks, 2002). If the station spacing is too large the data will not adequately reflect steeply dipping reflectors. The Nyquist sampling interval is one quarter of the wavelength in the host material and is expressed as

$$\Delta x = \frac{c}{4 f \sqrt{K}} = \frac{75}{f \sqrt{K}} ,$$

where f is the centre frequency (in MHz) and K is the dielectric constant of the host (Annan, 2003). For a centre frequency of 250 MHz and a dielectric constant of 4, the spatial sampling interval is 0.15 m. In our survey, a trace was acquired every 0.10 m. Depth of penetration is controlled by the attenuation of the material and system performance.

5.) Antenna separation for the Noggin 250 MHz system is a fixed value of 0.28 m.

6.) The establishment of a survey grid and coordinate system is important for the design of a survey. To reduce the number of survey lines, the lines should run perpendicular to the trend of the features under investigation. Line spacing is dictated by the degree of target variation in the trend direction. The line spacing for our surveys was chosen to be 1 m.

7.) The two antennae were parallel to each other and perpendicular to the direction of the survey line and primary energy propagation (this antenna orientation is sometimes called parallel-broadside).

DATA ACQUISITION

As previously mentioned, the 2003 3D GPR survey covered an ice surface of 25 m by 45 m (Figure 7) with 26 N-S lines set 1 m apart (one of the investigators actually wore skates to help with the traverses). These lines were acquired in a forward/reverse manner (every second line was collected in the reverse direction). The data were collected with Sensors and Software Inc.'s NOGGIN® 250 MHz system. As indicated, the centre frequency is 250 MHz and the antenna separation is 0.28 m. A trace was acquired automatically every 0.10 m as controlled by a counter on the SmartCart® wheel. The 2004 survey covered a surface of 20 m by 20 m (Figure 5), but with lines in orthogonal directions. In this case, we acquired a total of 42 GPR profiles, 21 lines on the E-W direction (X axis) and 21 lines on the N-S direction (Y axis). The NOGGIN® system was again used, but with a trace acquired every 0.05 m.
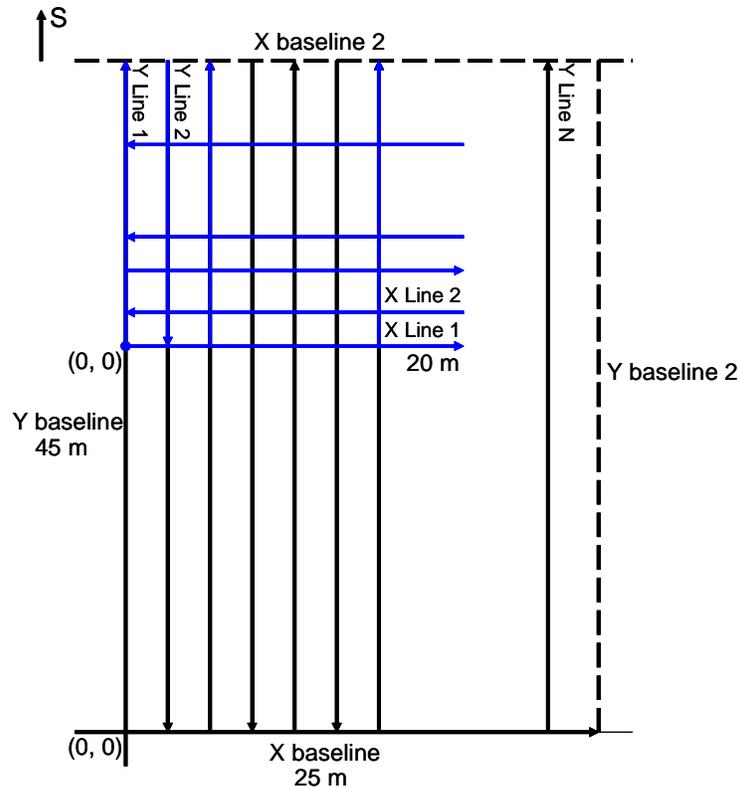
FIG. 7. The grid surveying pattern on the lagoon at Bowness Park. The area covered by the 2004 survey (20 m by 20 m) is represented in blue.

VELOCITY ANALYSIS SURVEYS

To transform the two-way travel time from reflection profiling into depth, the propagation velocity of electromagnetic energy through the profiled sediment has to be determined. An accurate radar velocity is critical for determining the depth of reflectors.

The propagation velocity can be determined in three ways: direct depth measurements, common-midpoint (CMP) velocity surveys and point-source reflections analysis, where the velocity is determined using the shape of diffraction patterns produced when profiling over point-source reflectors (Moorman et al., 2003).

A non-destructive way of determining velocity (as opposed to the straight forward process of drilling or digging) is a CMP survey. In this type of survey, the spacing between the transmitter and the receiver is successively increased with each step, while the antennae are centered on the same point (Figure 8). The results are used to obtain an estimate of the radar signal velocity versus depth in the ground by measuring the change of the two-way travel time to the reflections. Results from CMP sounding are a plot of antennae separation (distance) versus time. The dominant wavefronts which are normally observed are the direct airwave and then the direct ground wave, followed by any reflected and refracted radar waves. The slope of the lines is inversely proportional to the velocity.
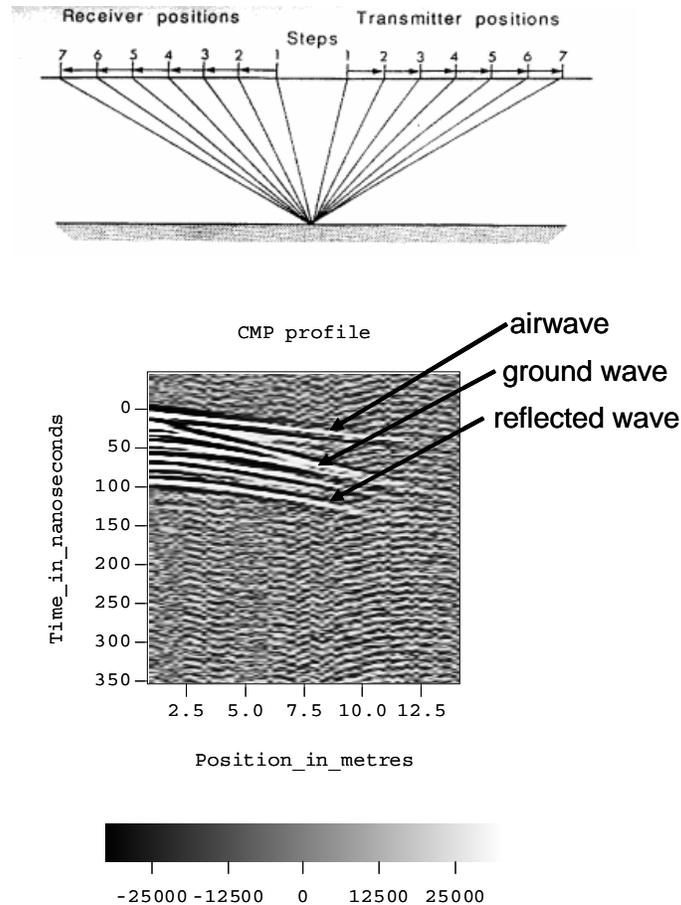
FIG. 8. The CMP procedure used to determine the electromagnetic propagation velocity of the near-surface sediments. An example from Bowness Park, Calgary of a CMP profile used to calculate the near-surface velocity. Pulse Ekko 4 system, with separate antennae of 100 MHz, was used to acquire this profile**.**

The CMP analysis program processes a CMP file by stacking the data at different velocities across lines or hyperbolic curves. When the traces are stacked at the correct velocity, they will add together constructively and produce high amplitudes. A plot of the stacked data allows us to match the highest amplitudes with a velocity value.

The near-surface velocity measurements were calculated from CMP surveys with the initial antennae separation of 1 m and steps of 0.2 m. The length of the survey line was 14 meters. This CMP gather, acquired on frozen ground near the lagoon, gave velocities from 0.14 m/ns in the very near surface (10 ns) to 0.1 m/ns at several meters depth (the event at 100 ns) (Figure 9). On the same figure we identify the airwave with a velocity of 0.3 m/ns.
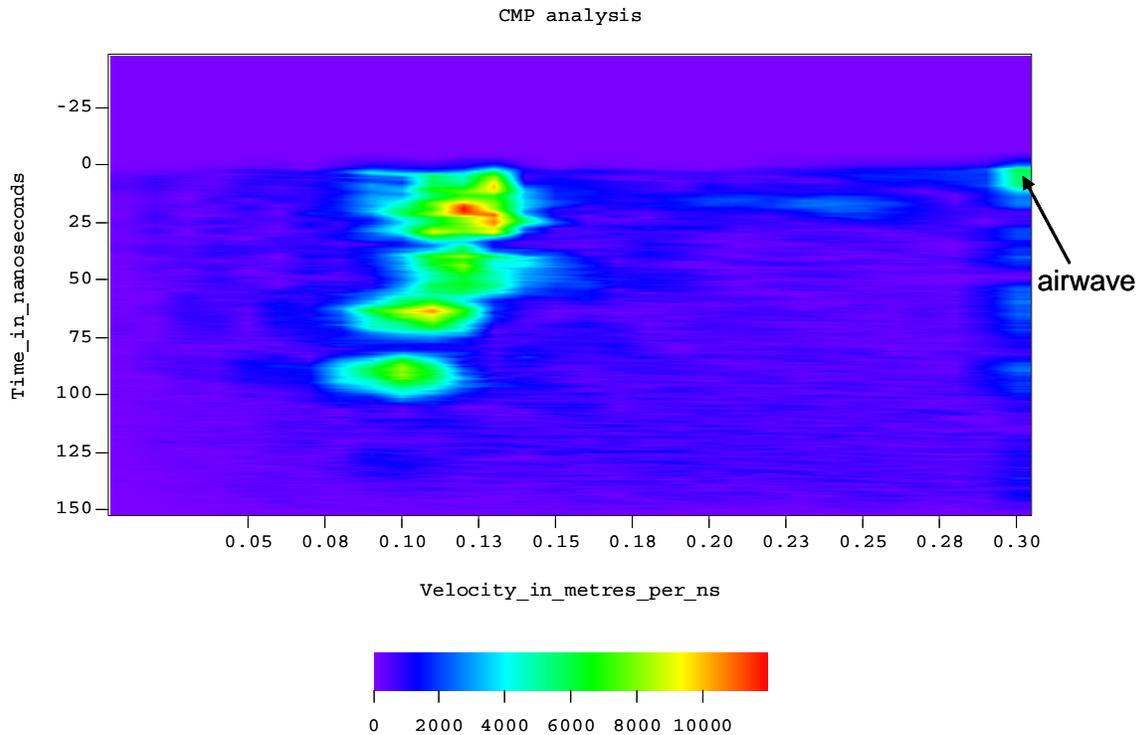
CMP analysis

FIG. 9. Velocity analysis from a CMP gather adjacent to the lagoon. The airwave has a velocity of 0.3 m/ns. The events between 10 and 100 ns have velocities varying between about 0.14 m/ns and 0.1 m/ns.

DATA ANALYSIS

The first stage in the analysis of the radar profile is to identify the origin of the reflections, which means to determine whether the interfaces indicated represent actual changes in the subsurface or interferences. A common interference is represented by responses which give rise to the hyperbolic features on GPR records. These are classic signatures of localized features such as pipes, cables, or other objects that are spatially limited. We encountered the presence of such features on the lines acquired adjacent to the lagoon, on frozen ground, as well as on the lines acquired over ice (Figure 10).

On lines 0 and 4, which are parallel lines, we identify diffraction hyperbolas. This usually indicates a point or line target (buried utilities, likely a pipe in this case). We also notice a clear reflection horizon at 44 ns on both lines (Figure 10), which we interpret as being the bedrock. Assuming a velocity of 0.1 m/ns, we calculate the depth of bedrock at 2.2 m

$$d = \frac{v \times t}{2},$$

where d is the depth in meters, v is the velocity of the radar wave through the material, in m/ns, and t is the two-way travel time, in nanoseconds).
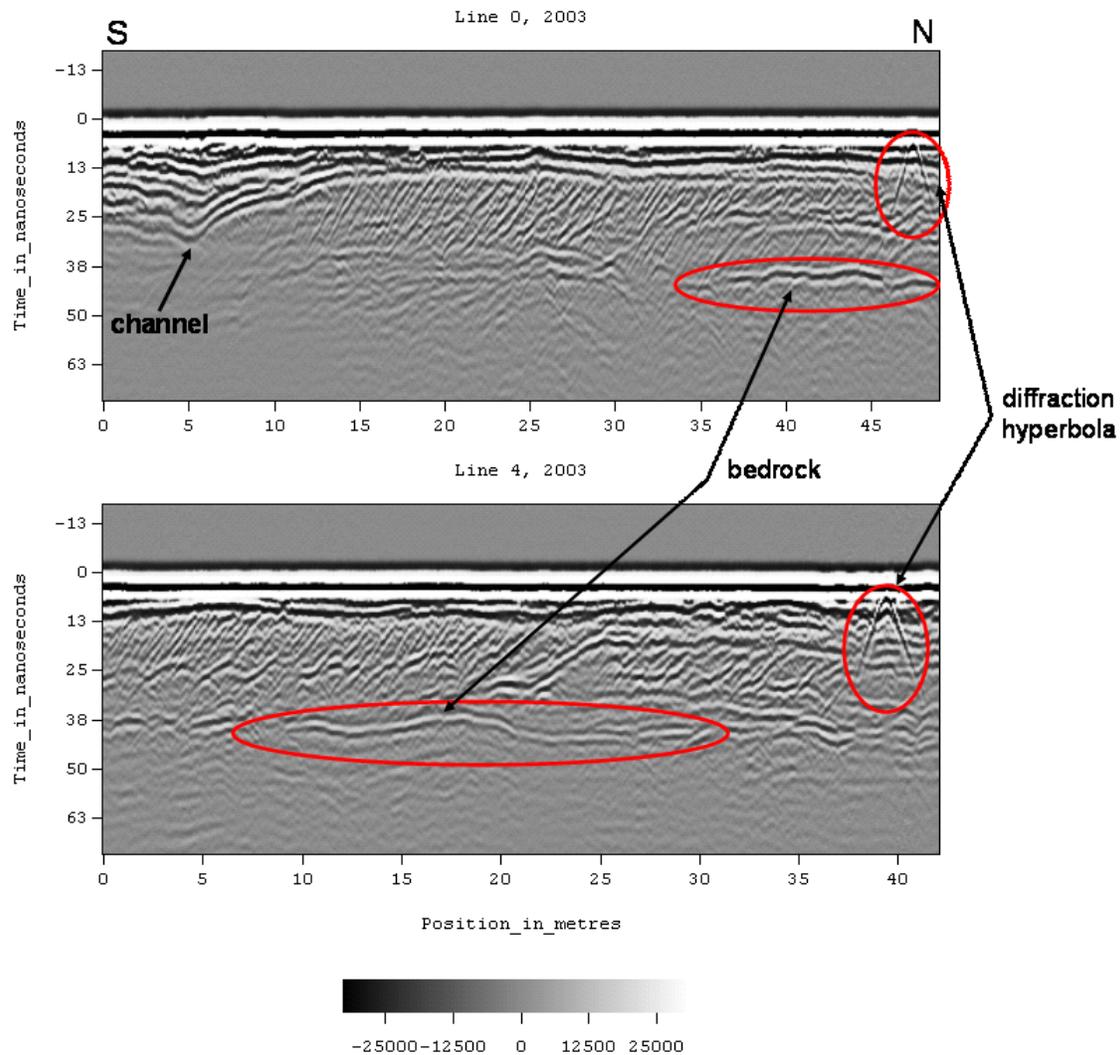
FIG. 10. Two parallel lines acquired adjacent to the lagoon. On the north side of the time section we identify a diffraction hyperbola, which indicates a point target (underground utilities). We also interpret the bedrock at 44 ns.

The raw GPR field data acquired were of reasonably good quality on their own. Nonetheless, we used GPR data processing procedures as outlined by various authors (e.g. Young et al., 1995, Fisher et al., 1996, Peretti et al., 1999) to further enhance the signal. These steps included: temporal filtering ("de-wowing") to remove very low-frequency components, time gain (an automatic gain control) to compensate for the rapid attenuation of the radar signal and to enhance deeper reflectors, and background subtraction to remove the air and ground wave from the time section and enhance shallow reflections.

The velocity value for ice, determined during acquisition by fitting a hyperbola to diffracting objects in the ice or just below it was 0.15 m/ns. By migrating the data with this velocity (Figure 11) we obtained a good image (i.e. the continuity of the reflectors increased). However, the diffractions were not collapsed.
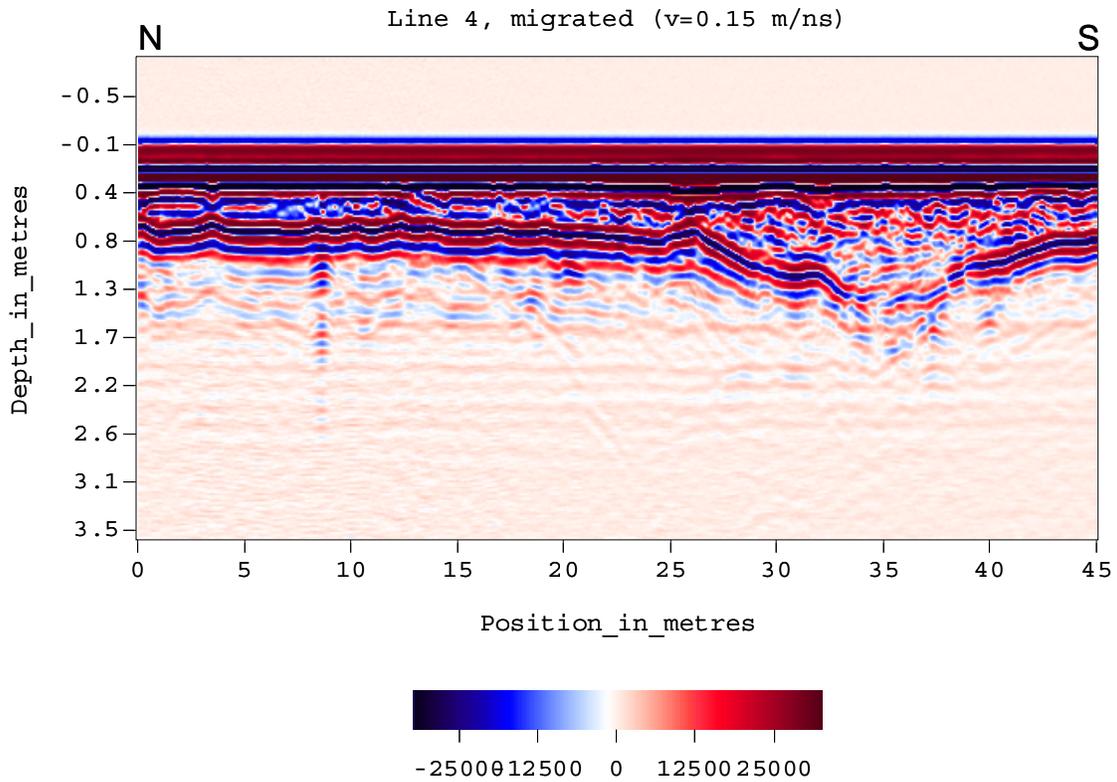
FIG. 11. A 2D line from the survey acquired over the frozen lagoon at Bowness Park, Calgary. The data were migrated with a velocity of 0.15 m/ns. The bottom of the ice is interpreted at 0.42 m depth.

We also used this velocity to map the section to depth and interpret the event at 0.42 m to be the ice bottom. Holes augured through the ice gave a thickness of about 0.4 m. The maximum depth of penetration of the reflected GPR signals is about 2 m, based on an average velocity of 0.11 m/ns and 40 ns two-way travel time.

By migrating our data with different velocities (0.08 m/ns and 0.1 m/ns) we were able to better image the deeper sediments (Figure 12).
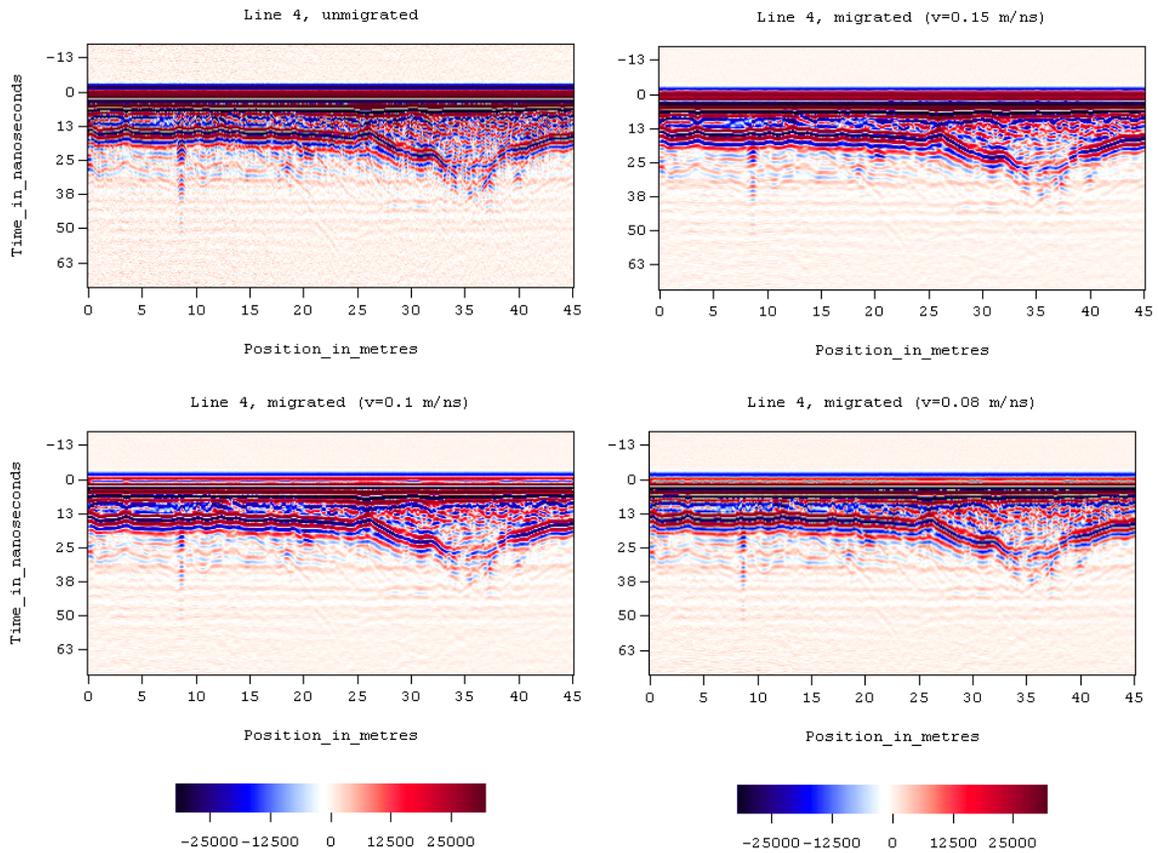
FIG. 12. A 2D line from the survey acquired over the frozen lagoon at Bowness Park, Calgary migrated with velocities of 0.15 m/ns, 0.1 m/ns, and 0.08 m/ns.

From three time slices (at 5 ns, 18 ns, and 26 ns two-way travel time), we were able to determine some subsurface structures. In particular, we can see detail at the bottom of the ice layer as well as the shape and orientation of the channel (Figure 13). On the time slice at 5 ns (the bottom of the ice layer) we can identify structures that follow the shape and orientation of the channel.
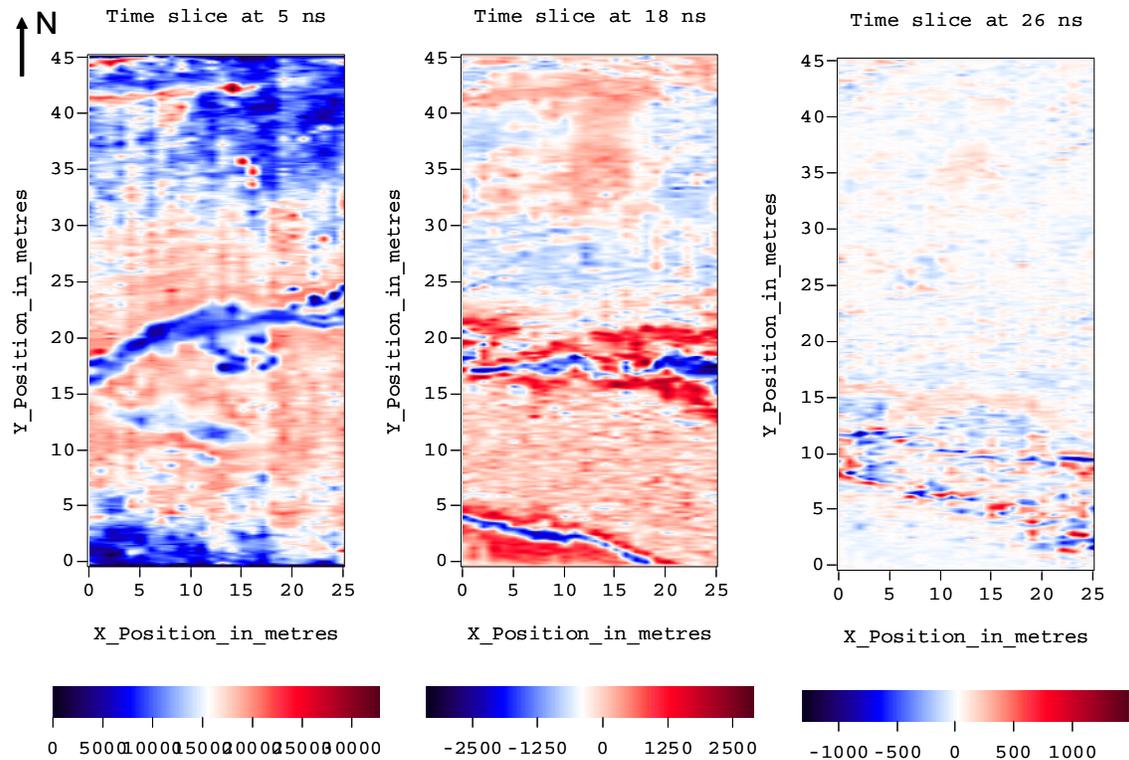
FIG. 13. Time slices of the 3D data acquired on the ice at Bowness Park. Amplitude increases from black to red. On the first slice at 5 ns, we are in the region of the bottom of the ice. The channel identified on the 3D cube is well mapped on the time slices.

We further analyzed this channel by computing time slices for the 16 ns to 26 ns interval. As we can see in these images (Figure 14), we first identify the channel-like features at 17 ns and they are hardly seen below 25 ns. This indicates that the channel is present for an interval of 8 ns. We were able to determine the thickness of the channel as being approximately 0.5 m (based on a velocity of 0.11 m/ns).
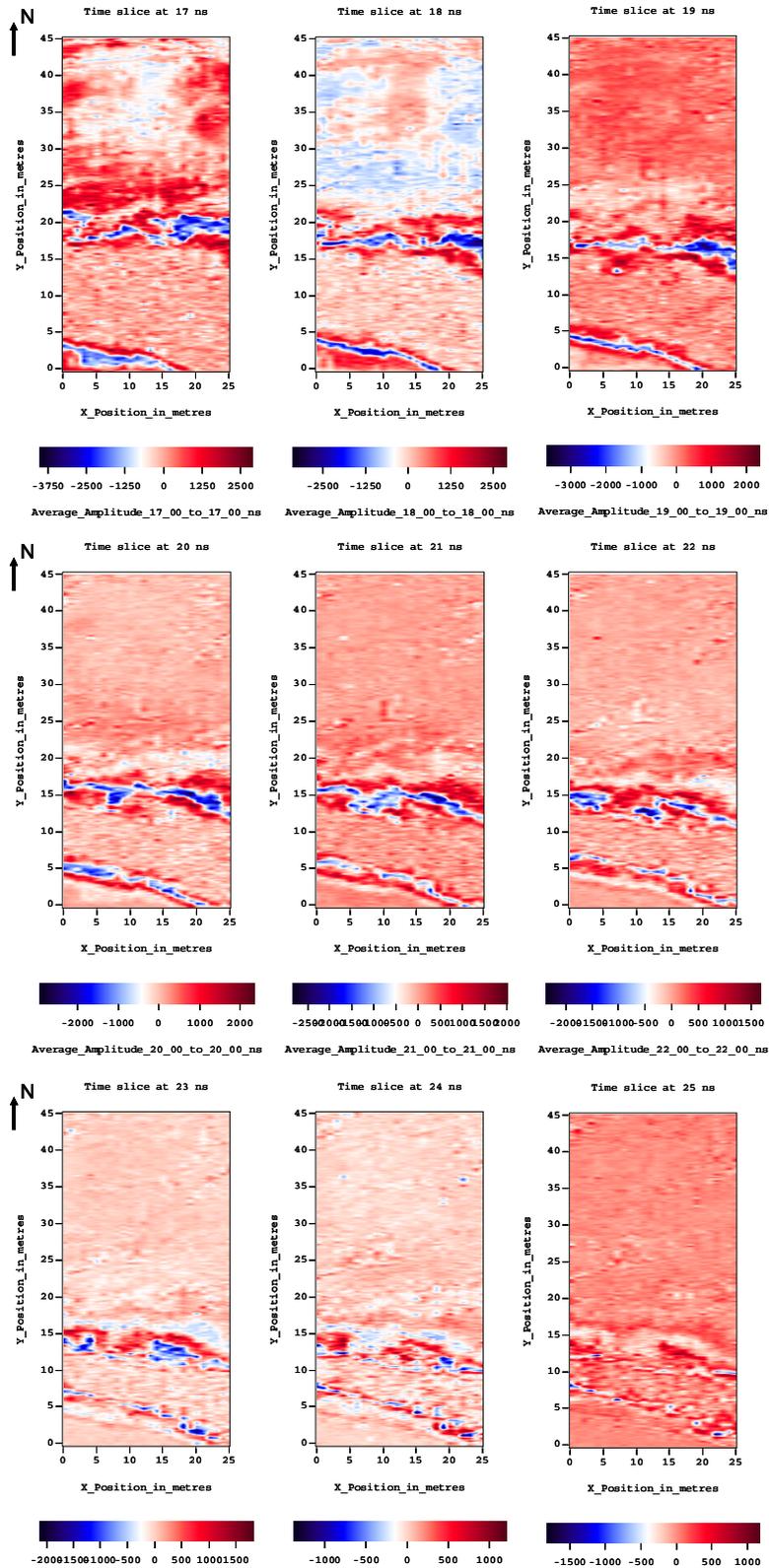
FIG. 14. Time slices computed for the 17 ns to 25 ns interval. Amplitude increases from black to red. We interpret a channel with a NW-SE orientation**.**

CONCLUSIONS

The GPR investigation over the frozen lagoon in Bowness Park, Calgary was useful in determining the thickness of the ice (about 0.4 m) and imaging fluvial structures beneath the ice. Velocity of the radar waves through ice was determined to be approximately 0.15 m/ns and the maximum depth from which we have information was approximately 2 m (using the deepest coherent reflections and a velocity of 0.11 m/ns).

We identified and mapped a paleochannel beneath the ice, with a NW-SE orientation and a thickness of about 0.5 m (also based on a velocity of 0.11 m/ns). On the lines acquired over the frozen land adjacent to the lagoon we interpreted the depth to the bedrock to be approximately 2.2 m (44 ns).

ACKNOWLEDGEMENTS

REFERENCES

Annan, A.P., 2003, Ground penetrating radar principles, procedures, and applications: Sensors & Software Inc.

Davis, J.L. and Annan, A.P., 1989, Ground-penetrating radar for high-resolution mapping of soil and rock stratigraphy, Geophysical Prospecting, **37**, 531-551.

Fisher, S.C., Stewart, R.R., and Jol, H.M., 1996, Processing ground penetrating radar (GPR) data, J. Environmental and Engineering Geophysics, **1**, 89-96.

Keary, P. and Brooks, M., 2002, An introduction to geophysical exploration, Blackwell Scientific Publications, Boston, Massachusetts, 3rd Edition.

Moorman, B.J., Robinson, S.D., and Burgess, M.M., 2003, Imaging periglacial conditions with ground-penetrating radar, Permafrost and Periglacial Processes, **14**, 319-329.

Moran, S. R., 1986, Surficial geology of the Calgary urban area, Alberta Research Council, Bulletin 53.

Olhoeft, G.R., 2000, Maximizing the information return from ground penetrating radar: J. Applied Geophysics, **43**, 175-187.

Osborn, G. and Rajewicz, R., 1998, Urban Geology of Calgary: Geological Association of Canada, Special Paper 42, Urban Geology of Canadian Cities, 93-115.

Peretti, W.R., Knoll, M.D., Clement, W.P., and Barrash, W., 1999, 3D GPR imaging of complex fluvial stratigraphy at the Boise hydrogeophysical research site, in Proc. of the Symposium on the Application of Geophysics to Engineering and Environmental Problems, 18-18 March 1999, Oakland, CA.

Young, R.A., Deng, Z. and Sun, J., 1995, Interactive processing of GPR data: The Leading Edge, **14**, 275-280.